



# Chemical abundances in AGN : X-ray/UV campaign on Mrk 279

Nahum Arav

Center for Astrophysics and Space Astronomy, University of Colorado, 389 UCB, Boulder  
CO 80309-0389, e-mail: arav@colorado.edu

**Abstract.** We present the first reliable chemical abundances determination in an AGN outflow. The abundances are extracted from the deep and simultaneous FUSE and HST/STIS observations of Mrk 279. This data-set is exceptional for its high signal-to-noise, unblended doublet troughs and little galactic absorption contamination. These attributes allow us to solve for the velocity dependent covering fraction, and therefore obtain reliable column density for many ionic species. For the first time we have enough such column densities to simultaneously determine the ionization equilibrium and abundances in the flow. Our analysis use the full spectral information embedded in these high-resolution data. Slicing a given trough to many independent outflow elements yields the extra constraints needed for a physically meaningful abundances determination. We find that relative to solar the abundances in the Mrk 279 outflow are: carbon  $2.2 \pm 0.7$ , nitrogen  $3.5 \pm 1.1$  and oxygen  $1.6 \pm 0.8$ .

**Key words.** galaxies: active — galaxies: abundances — galaxies: individual (Mrk 279) — galaxies: Seyfert — line: formation — quasars: absorption lines

## 1. Introduction

Active galactic Nuclei (AGN) are chemically evolved environments. The spectrum of the highest redshift quasar ( $z=6.4$ ) is very similar to those of quasars in the local universe (3C273  $z=0.13$ ) (Fan et al 2004), suggesting that chemical enrichment of AGN environments operates on short cosmological time-scales. This feature makes local easy-to-study AGN a good probe of chemical processing when the universe was less than 20% of its current age.

There are two main tracks for determining abundances in AGN: Broad emission lines (BELs) are seen in most AGN and are known to be formed in close proximity of the nucleus (0.01–0.1 pc.; Kaspi et al). Due to the brightness of the objects, BELs are relatively easy to

measure. For these reasons much effort was put into trying to determine abundances in AGN by studying the relative strength of BELs in individual as well as composite spectra (e.g., Shields the Baldwin & Netzer 1978; Hamann & Ferland 1992; Ferland et al. 1996 Dietrich et al. 1999, 2003). These studies suggest that the metallicity of the BEL region (BELR) is super solar. However, BEL abundances studies are fraught with several unresolved obstacles. The BELR is spatially stratified and likely to have a wide range of densities and temperatures. Therefore, different BELs can arise from different regions, which cast doubts on the validity of BEL ratios as abundances indicator. Radiation transfer inside the opaque BEL material is a difficult problem that further com-

plicates interpreting observed BEL ratios. The relative abundance of hydrogen, which is the corner stone to all metallicity determinations, is especially affected by highly opaque radiation transfer.

The second track for determining abundances is using absorption lines associated with AGN outflows. AGN outflows are evident by resonance line absorption troughs, which are blueshifted with respect to the systemic redshift of their emission counterparts. In Seyfert galaxies velocities of several hundred  $\text{km s}^{-1}$  (Crenshaw et al. 1999; Kriss et al. 2000) are typically observed in both UV resonance lines (e.g., C IV  $\lambda\lambda 1548.20, 1550.77$ , N V  $\lambda\lambda 1238.82, 1242.80$ , O VI  $\lambda\lambda 1031.93, 1037.62$  and Ly $\alpha$ ), as well as in X-ray resonance lines (Kaastra et al. 2000, 2002; Kaspi et al. 2000, 2002). Similar outflows (often with significantly higher velocities) are seen in quasars which are the luminous relatives of Seyfert galaxies (Weymann et al. 1991; Korista, Voit, Morris, & Weymann 1993; Arav et al. 2001a). Distances of the outflows from the central source can range from smaller than BELR distances (QSO 1603; Arav et al 2001); tens of pc. (NGC 3783; Gabel et al 2005); 1000 pc. (QSO 1044; de Kool et al 2001). Therefore, in many cases the outflows are associated with material in close proximity to the AGN, and can be used as diagnostics for the chemically enriched environment at the center of galaxies.

A main obstacle in determining abundances using outflow absorption lines is obtaining reliable measurement of the absorption column densities from the troughs. Using the doublet method (Barlow 1997, Hamann et al 1997) we have shown that in many cases the shapes of the troughs are almost entirely due to changes in the line of sight covering as a function of velocity, rather than to differences in optical depth (Arav et al. 1999b; de Kool et al. 2001; Arav et al. 2001a). Gabel et al. (2003) show the same effect in the outflow troughs of NGC 3783, as does Scott et al. (2004) for Mrk 279. As a consequence, the column densities inferred from the depths of the troughs are only lower limits.

In order to measure reliable column densities we found it necessary to use a two step combination: First, we developed analysis methods that can disentangle the covering factors from the optical depth (Gabel et al. 2003, 2005). Second, these methods depends on having high-resolution ( $\gtrsim 20,000$ ) and high signal-to-noise ( $S/N \gtrsim 20$ ) spectral data of outflow troughs. Furthermore, we critically rely on fully-resolved uncontaminated doublet and multiple troughs. Mrk 279 is the optimal target for such analysis, since it allowed to obtain data with the above specification on the C IV, N V, and O VI doublet, as well as on several Lyman series troughs. The latter are crucial for any abundances determination (see § 4.1).

It is important to note that our partial covering models are velocity dependent and therefore the extracted column densities are also a function of velocity. This allows us to obtain the maximum possible amount of physical information for a given spectroscopic resolution. This feature is key in determining the abundances and limiting their errors.

In this paper we present the determination of chemical abundances in the AGN outflow emanating from Mrk 279, using the high-quality simultaneous UV data sets from HST/STIS and FUSE. In § 2 we describe our photoionization analysis, including: the column density data set; photoionization grid models and velocity dependent grid models. In § 3 we use the velocity dependent information to determine the chemical abundances in the outflow. In § 4 we discuss our results.

## 2. Photoionization Analysis

### 2.1. The Mrk 279 Data Set

On May 2003 we obtained simultaneous X-ray and UV observations of the Mrk 279 AGN outflow. (Description of the UV observations is found in Gabel et al. 2005, and the X-ray observations in Costantini et al. 2006.) The 92 ksec FUSE data yielded the highest quality O VI trough-spectrum of any AGN outflow to date, and the 16 orbits HST/STIS/E140M observation yielded high quality N V troughs.

The combined HST/FUSE spectrum gives high signal-to-noise Ly $\alpha$ , Ly $\beta$  and Ly $\gamma$  troughs.

In Gabel et al (2005) we used a global fitting technique to extract three velocity Dependant quantities from the data: Continuum covering factor, BELR covering factor and column densities  $N_{ion}$  for all the detected ions. An important finding was that the outflow fully cover the continuum both for the Lyman series troughs and for the CNO doublets. In this paper we refine the  $N_{ion}$  measurements by using this finding. Once the continuum coverage is known to be 100%, the doublet equations are reduced to two unknowns (BELR covering factor and optical), which we can solve for since we have two residual intensity equations. These solutions are more physical and their errors are easier to estimate.

## 2.2. Photoionization Modeling and SED

We use simple-slab photoionization models (using the code CLOUDY; Ferland 1996). Such models are commonly used in the study of quasar outflows (e.g., Weymann, Turnshek, & Christiansen 1985; Arav & Li 1994; Hamann 1996; Crenshaw & Kraemer 1999; Arav et al. 2001b, Gabel et al. 2006) and assume that the absorber consists of a constant density slab irradiated by an ionizing continuum. The two main parameters in these models are the thickness of the slab as measured by the total hydrogen column density ( $N_H$ ) and the ionization parameter  $U$  (defined as the ratio of number densities between hydrogen ionizing photons and hydrogen in all forms).

## 2.3. Velocity-Dependent Grid Models

We base our photoionization analysis, and ultimately the abundances determination on the grid models approach created by Arav et al. (2001a). For a given  $N_{ion}$  we ran a grid of models spanning three orders of magnitude in both  $N_H$  and  $U$ . For these models We use the Mrk 279 SED described above and assume solar abundances. We determine which combinations of  $N_H$  and  $U$  will create the observed  $N_{ion}$  and than plot the ion-curve: the lucos of these

points on the  $N_H/U$  plane. We do that for each measured  $N_{ion}$ . Ideally, a single value of  $N_H$  and  $U$  should be able to reproduce all the  $N_{ion}$  constraints. On the  $N_H/U$  plane this will be represented by the crossing of all the ion-curves at a single point.

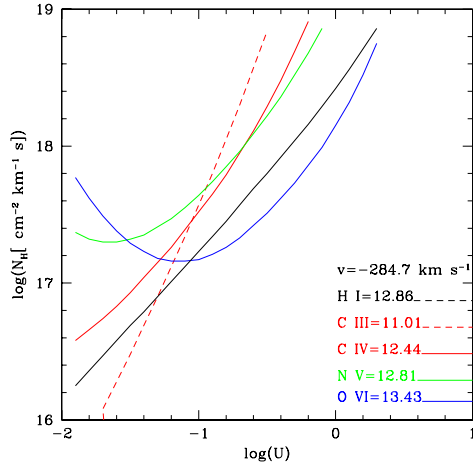
A new feature that adds considerable diagnostic power to these models, is their velocity dependence. Since the  $N_{ion}$  measurement are for a specific velocity we obtain a grid model for each element of resolution along the trough. There is no a-priori reason why material flowing in different velocities should have the same ionization structure or have the same column density per unit velocity (see § 4.1). Separating the absorption trough to individual resolution elements therefore allows for a more accurate solution of the ionization structure of the flow, and as we show below, is the key for meaningful abundances determination.

Figure 1 shows the grid model for the the resolution-element centered around the  $-285$  km s $^{-1}$  outflow velocity. All the measured ions are represented. The upper limits from Si IV, S IV, S VI and C II, do not add meaningful constraints and are consistent with the results of our analysis. An important advantage over the analysis of the PG 0946+301 spectra (Arav et al. 2001), is that all the  $N_{ion}$  shown on Fig. 1 are actual measurements and not lower limits, as was the case for most ions in PG 0946+301.

## 2.4. Measurement Errors and $\chi^2$ Analysis

In measuring the  $N_{ion}$  for the outflow troughs in Mrk 279 we accounted for most of the systematic issues that plagued previous measurements. Unblended doublet and multiplet troughs were used, without which reliable outflow  $N_{ion}$  cannot be measured in principle. Both the continuum and BELR covering factors were taken into consideration, and  $N_{ion}$  as a function of velocity was extracted. We therefore possess the first comprehensive set of reliable  $N_{ion}$  measurements for an AGN outflow.

Extracting meaningful constraints on the ionization equilibrium and abundances from the measured  $N_{ion}$  requires having a reliable data base of the associated errors. Estimating



**Fig. 1.** Curves of constant ionic column density plotted on the plane of total hydrogen column density ( $N_H$ ) per unit velocity of the slab vs. the ionization parameter of the incident radiation ( $U$ ), using solar abundances and an SED tailored for these specific observations of Mrk 279. The inserted Table shows measured  $\log(N_{ion})$  [per unit velocity] for the resolution-element centered around the  $-285 \text{ km s}^{-1}$  outflow velocity.

physical errors for the  $N_{ion}$  measurements is a complicated process that is fully described in Arav et al. (2006). Here we give a brief description of this process and a qualitative explanation for the different error values of the individual ions. For all ions except C III the fitting procedure simultaneously find the optimal covering factor and optical depth at a given velocity point. Once the optimal combination is found, we derive the formal error of the parameters (see Arav et al. 2006 for full discussion). It is very reassuring that the resultant flux deviation are quite similar to the empirical flux error both in the positive and negative directions.

In Fig. 2 we show the errors associated with the photoionization model presented in Fig. 1. O VI has the largest errors both because at that velocity it's troughs are nearly saturated, for that reason the assymetry in it's errors is also most pronounced. H I exhibits the smallest er-

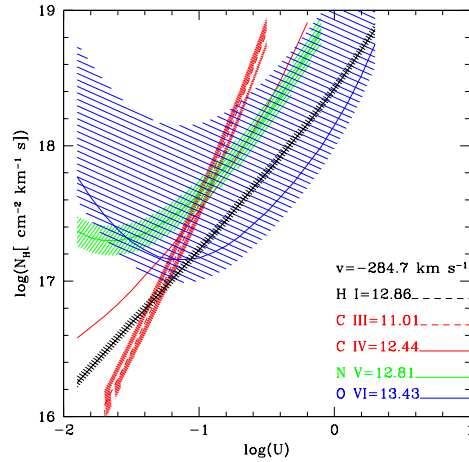


**Fig. 2.** Same as 1, but including  $1\sigma$  uncertainties, shown as shaded areas having the same color as their associated ion curve. For the sake of clarity, we omitted the  $1\sigma$  presentation for C IV. As a figure of merit, in this velocity plot the  $1\sigma$  interval for C IV touches the H I curve around  $\log(U) = -1.4$ .

rors, and therefore supplies the strongest constraint on the physical solutions for the outflowing gas. The H I errors are the smallest because the observations cover five Lyman series lines and the intrinsic optical depth ratio of the first three spans a factor of 18. This coupled with the fact that the Ly $\gamma$  trough is not close to saturation, yield tight constraints on the column density. In contrast the intrinsic optical depth ratio between the members of the each CNO doublet is 2, yielding significantly less stringent constraints on their  $N_{ion}$ . C III is a singlet and therefore we had to make an assumption regarding it's covering fraction. Once we assumed the C III coverage to be the same as C IV we derived tight constraints on it's  $N_{ion}$  since the trough was far from saturation. Finally, a contributing factor for the larger errors of the CNO doublets is that flux errors are associated with both doublet components while often the difference between the two residual intensities is small compared to the flux values themselves.

We are now in position to ask the first important physical question: Do the ion-curves in Fig. 2 allow for an acceptable solution for the ionization equilibrium for this particular velocity-slice of the outflow? That is, is there a combination of  $N_H$  and  $U$  That will satisfy all the ion-curve constraints. It is evident from Fig. 2 that this is not the case, as the error stripes for H I and N v do not overlap on this grid-model plot. A physical solution cannot be obtain for this velocity-slice of the outflow assuming solar abundances. In Fig. 3 we show the formal  $\chi^2$  solution for the best fit values of  $N_H$  and  $U$  of this velocity-slice. The reduced  $\chi^2 = 5.4$ , formally shows that the model does not yield a statistically valid fit for the data. A similar situation occurs in almost all other velocity-slice that include the same ion-curves.

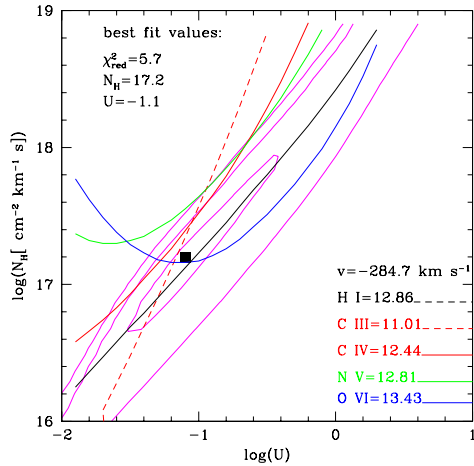


**Fig. 3.** Similar to Fig. 1 over-plotted with reduced  $\chi^2$  contours (at 12.5,50,112) for an  $N_H, U$  solution (purple lines). Position of the formal solution is marked by the filled square and the best fit values are shown at the top left corner. From the large value of the reduced  $\chi^2$  it is evident that there is no acceptable  $N_H, U$  solution for this solar abundances model.

### 3. Abundances Determination

#### 3.1. Method

The most plausible way to obtain a physical solution for  $N_H$  and  $U$  in Fig. 2 is to drop the assumption of solar abundances. On our parameter space plots an increase in abundance is equivalent to lowering the entire related ion-curve, since less  $N_H$  is needed for the same amount of the said element. We can see from Fig. 2 that if the nitrogen abundance is 3 times higher than solar, the N v ion-curve will be lower by the same amount and the error stripes for H I and N v will comfortably overlap in parts of the parameter space.

For one velocity slice we can always achieve a perfect solution (exact crossing of the ion curves) by allowing the CNO abundances relative to hydrogen to be free parameters. Such a solution might be suggestive, but it is considered weak since we use three free parameters to make the 5 ion-curves cross at the same point. As can be seen in 1, this is always the case. As long as we specify the value of  $U$  to be that of the C III and C IV ion-curves crossing point, the three free abundances parameters allow us to bring all CNO ion-curves to meet at that  $U$  value on top of the H I curve.

The way to obtain a robust rather than suggestive abundances determination for the outflow is to use the velocity information. So far we have only dealt with a single velocity-slice. It is reasonable to expect that each velocity-slice will have an independent ionization solution, i.e., it's own  $N_H, U$  values. The number density and column density of the outflow at each resolution element are determined by the flow's dynamics, which can be quite complicated (Proga 2005). However, it is likely that an outflow component would have the same abundances at all velocities. Therefore, the assumptions we make are: 1) each velocity-slice has an independent  $N_H, U$  ionization solution; 2) all velocity slices of the same outflow component have the same chemical abundances.

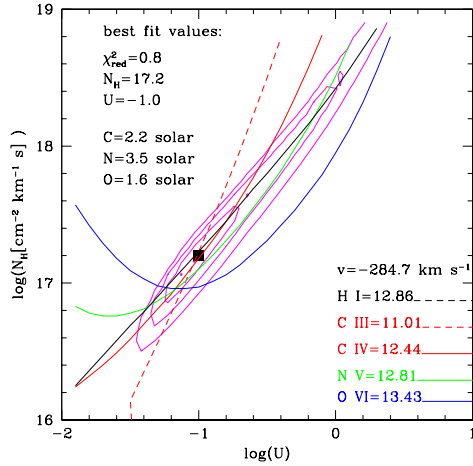


**Fig. 4.** Similar to Fig. 3 for the best global abundances solution. Reduced  $\chi^2$  contours are plotted at 1.2, 4.8 and 11) for an  $N_H$ ,  $U$  solution (purple lines). Position of the formal solution is marked by the filled square and the best fit values are shown at the top left corner. The reduced  $\chi^2$  gives an acceptable  $N_H$ ,  $U$  solution for this abundances solution.

### 3.2. Results

We obtain the best fit for the following set of CNO abundances (relative to solar) carbon=2.2, nitrogen=3.5 and oxygen=1.6. For this model  $\chi^2 = 47.5$  for 41 degrees of freedom, or a reduced  $\chi^2$  of  $\chi^2_{red} = 1.16$  (see Arav et al. 2006). In Fig. 4 we show the formal  $\chi^2$  solution for the best fit values of  $N_H$  and  $U$  of the same velocity slice shown in Fig. 3. The reduced  $\chi^2 = 0.8$ , formally shows that the model yield a statistically valid fit for the data. A similar situation occurs in most other velocity-slice that include the same abundances solution.

We calculate the model-independent errors associated with these abundances determination by finding the 90% single parameter confidence obtained from changing only the said abundance while keeping the others fixed (following Press et al 1989 and Taylor 1997). The results are shown in Table 1. One can also find a model-dependent error-estimate based on the physical expectation that the ratio of

C/H and O/H are proportional to each other while  $N/H \propto (O/H)^2$ . For this model the 90% confidence level for nitrogen is only slightly lowered but the error bars on the oxygen and carbon abundances shrink shrink by 60% and 50% respectively.

Thus, carbon and oxygen are enhanced by a factor of  $\approx 2$  relative to solar values, while nitrogen is enhanced by a factor of 3-4. In agreement with the  $Z^2$  scaling indicative of enhanced secondary production in massive stars (Hamman et al 1999, and references therein)

## 4. DISCUSSION

### 4.1. Robustness of the Abundances Determination

We argue that the work described here is the first reliable abundances determination in AGN outflows. To support this claim let us review what is necessary for deriving reliable abundances in the outflows, and how well did this project meet these requirements. In § 5.3 we describe how other previous and current effort fall short of satisfying these necessary conditions.

Determining the ionization equilibrium and abundances (IEA) in AGN outflow depends crucially on obtaining reliable measurement of the absorption  $N_{ion}$  from the observed troughs. As described in the Introduction and elsewhere (Arav et al. 1999b; de Kool et al. 2001; Arav et al. 2001a; Gabel et al. 2003; Scott et al. 2004) solving for the velocity-dependent covering fraction is crucial for obtaining reliable  $N_{ion}$  from the troughs. Column densities inferred using other techniques (curve of growth, apparent optical depth and Gaussian modeling) suffers from large systematic uncertainties and many times can only be used as lower limits. We have developed state-of-the-art velocity-dependent methods to determine the covering fraction of both the continuum and BELR as well as the real optical depth (Gabel et al 2005 and this work). To implement these methods a suitable data-set must have the following attributes:

1) Spectral resolution larger than 20,000 in order to allow for velocity-dependent analysis

**Table 1.** ABUNDANCES OF THE MRK 279 OUTFLOW RELATIVE TO SOLAR

element	abundance	upper error	lower error
carbon	2.2	0.7	0.7
nitrogen	3.5	1.1	1.1
oxygen	1.6	0.7	0.8

across the troughs. FUSE and the Echelle gratings on board HST give us sufficient resolution.

2) To enable a meaningful covering factor analysis of the CNO doublets, the S/N of the data must be  $\geq 20$  for the above resolution. Very few data sets in the literature achieve this S/N level since it requires roughly  $\geq 15$  HST/STIS orbits and  $\geq 100$  ksec of FUSE exposure time on the brightest AGN outflow targets.

3) The Data-set must cover troughs from enough ions to be useful for IEA determinations. At the minimum we need to cover the CNO doublets and three or more of the Lyman series troughs. The latter is a crucial requirement since abundances cannot be determined without an accurate measurement of H I column density. Only a combination of FUSE and HST can cover the needed troughs.

4) The troughs associated with different doublet components must be unblended. Otherwise it is impossible to use extract covering factor and the derived  $N_{ion}$  are reduced to lower limits. Similarly, the outflow troughs cannot be contaminated with significant galactic absorption.

5) FUSE and HST/STIS coverage must be near-simultaneous, preferably within the same month. Seyfert outflow troughs are known to show considerable changes over time scales of more than several months (e.g., NGC 3783 Gabel et al 2004; Mrk 279, Scott et al 2004). Any combined analysis of the full data set must rely on no changes in the absorption between the different epochs.

The deep and simultaneous FUSE and HST/STIS observations of Mrk 279 is the only existing data set that satisfy all these requirements. Therefore, our measurements yield the

first sufficient set of reliable  $N_{ion}$  to allow for a physical determination of the IEA in AGN outflows.

Our next step was to infer the physical conditions of the absorbing gas using these  $N_{ion}$  measurements. Here we introduced an analysis method that use the full information imprinted on these high-resolution data. (In parallel Gabel et al. 2006 are using similar techniques on the spectrum of QSO J2233-006) Instead of integrating the  $N_{ion}$  across a kinematic component we treat each resolution element separately. Physically, this approach is justified since elements of the flow that are separated by more than several  $\text{km s}^{-1}$  represent physically-separated and sonically-disconnected regions. In this way, instead of having constraints on the physical conditions in one kinematic component, we obtain constraints on 15 separate regions. We therefore do not have to use the implicit assumption that the ionization equilibrium is constant across a given component.

For one kinematic component given the set of measured  $N_{ion}$ , it is always possible to find a set of CNO abundances that will produce a perfect photoionization solution. It is therefore impossible to assess the physical significance of such a solution. The situation is different for constraining 15 separate regions. We rely upon two plausible physical assumptions, that the individual  $U$  and  $N_H$  can vary from one region to another, and that the abundances across these regions is constant. This allows us to obtain tight constraints for the individual CNO abundances as described in § 3.4. We spent a great deal of effort to derive physically meaningful errors on our  $N_{ion}$  measurements. It is very reassuring that the excellent statistical fit of our

abundance model (reduced  $\chi^2 = 1.16$ ) was achieved without any re-adjustments of these errors.

#### 4.2. Possible Caveats

As described above, we invested a large effort in developing and utilizing analysis techniques that solved for two separate covering factors and the optical depth as a function of velocity. An important question in this context is how valid is the assumption of a rigid absorbing-material distribution (essentially a step-function) assumed by the partial covering model? Would an inhomogeneous distribution of absorbing material across the emission source (de Kool, Korista & Arav 2002) can yield a good alternative to the partial covering model? In Arav et al. (2005) we tested inhomogeneous absorber models on the Mrk 279 data set, where the three high quality Ly $\alpha$ , Ly $\beta$  and Ly $\gamma$  troughs provided the strongest constraints. We concluded that inhomogeneous absorber models that do not include a sharp edge in the optical depth distribution across the source are not an adequate physical model to explain the trough formation mechanism for the outflow observed in Mrk 279. This result supports to the use of partial covering models for AGN outflows

#### 4.3. Comparison With Other Outflow Metallicity Determinations

All IEA studies of Seyfert outflows prior to 2003 used  $N_{ion}$  measuring techniques that are inadequate for AGN outflows troughs: curve of growth, apparent optical depth and Gaussian modeling. The key importance of the covering factor was overlooked. Therefore, the IEA findings of these studies suffer from large unquantified systematic errors that can only be corrected to some extent by redoing the analysis using more accurate trough formation models. In many cases a reanalysis is unwarranted since one or more of the conditioned detailed in § 4.1 is not met: S/N of the data is insufficient (e.g., Fields et al 2005); Data does not cover troughs from enough ions to be useful for IEA

determinations. (e.g., Brotherton et al 2001) Doublet troughs are blended (e.g., NGC 4151, Kraemer and Crenshaw 2001)); Severe contamination with galactic absorption (e.g., NGC 3783, Gabel et al 2003); FUSE and HST/STIS coverage is not simultaneous.

A typical recent example is the Study of the Mrk 1044 outflow (Fields et al 2005), which has the following shortcomings: a) S/N of the FUSE data is too low to allow a covering-factor analysis. b) There is severe contamination with galactic absorption in the FUSE band, greatly affecting the measurements of the crucial Ly $\beta$  trough. c) FUSE and HST/STIS observations were taken 6 months apart allowing significant changes in the absorber to occur, while it is necessary to assume that no absorption change occurred for the sake of the photoionization analysis. d) There was no attempt to solve for the velocity dependent covering factor for the STIS observed C IV and N V, which introduces large errors in their  $N_{ion}$  determination. e) The main measured FUSE lines (O VI) are totally saturated, thus the derived O VI column density is only a lower limit. Most importantly, the main conclusion, that the outflow show metallicity of at least 5 times solar is greatly weakened by the fact that the Lyman series troughs are either heavily blended (Ly $\beta$ ), or of too poor quality (Ly $\gamma$ ) for analysis. A possible factor of 3 increase in the H I measurement is reasonable under these conditions and will make the photoionization model (see their Fig. 5) consistent with solar metallicity.

#### Acknowledgments

This work is based on observations obtained with *HST* and *FUSE*, both built and operated by NASA. Support for this work was provided by NASA through grants number *HST*-AR-9536, *HST*-GO-9688, from the Space Telescope Science Institute, which is operated by the Association of Universities for Research in Astronomy, Inc., under NASA contract NAS5-26555, and through *Chandra* grant 04700532 and by NASA LTSA grant 2001-029. The National Laboratory for Space Research at Utrecht is supported financially



by NWO, the Netherlands Organization for Scientific Research.

## References

- Arav, N., 1997 in Mass Ejection from AGN, ASP Conference Series, Vol. 128, ed. N. Arav, I. Shlosman, and R. J. Weymann, p. 208
- Arav, N., Korista, T. K., de Kool, M., Junkkarinen, V. T. & Begelman, M. C. 1999, *ApJ*, 516, 27. (1999a)
- Arav, N., Becker, R. H., Laurent-Muehleisen, S. A., Gregg, M. D., White, R. L., Brotherton, M. S., & de Kool, M. 1999, *ApJ*, 524, 566 (1999b)
- Arav, N., Brotherton, M. S., Becker, R. H., Gregg, M. D., White, R. L., Price, T., Hack, W. 2001, *ApJ*, 546, 140 (2001a)
- Arav, N., et al. 2001, *ApJ*, 561, 118 (2001b)
- Arav, N., Korista, T. K., de Kool, M., 2002, *ApJ*, 566, 699
- Arav, N., et al. 2005, *ApJ*, 620, 665
- Arav, N., et al. 2006, *ApJ*, submitted
- Barlow, T. A., 1997 in Mass Ejection from AGN, ASP Conference Series, Vol. 128, ed. N. Arav, I. Shlosman, and R. J. Weymann, p. 13
- Costantini, E., et al. 2006, in preparation
- Churchill, C. W., Schneider, D. P., Schmidt, M., Gunn, J. E., 1999, *AJ*, 117, 2573
- Crenshaw, D. M., Kraemer, S. B., Boggess, A., Maran, S. P., Mushotzky, R. F., Wu, C. C., 1999 *ApJ*, 516, 750
- de Kool, M., Arav, N., Becker, R. H., Laurent-Muehleisen, S. A., White, R. L., Price, T., Gregg, M. D. 2001, *ApJ*, 548, 609
- de Kool, M., Becker, R. H., Gregg, M. D., Arav, N., White, R. L., Korista, K. T., 2002, *ApJ*, 567, 58
- de Kool, M., Korista, K. T., Arav, N., 2002, *ApJ*, 580, 54 (dKKA)
- Gabel, J. R., et al. 2003, *ApJ*, 583, 178
- Gabel, J. R., Arav, N., Kaastra, J. S., et al. 2005, *ApJ*, 623, 85
- Ganguly, R., Eracleous, M., Charlton, J. C., & Churchill, C. W. 1999, *AJ*, 117, 2594
- Ganguly, R., Eracleous, M. C., Charlton, J. C., & Churchill, C. W. 1999, *AJ*, 117, 2594
- Hamann, F., Barlow, T. A., Junkkarinen, V., Burbidge, E. M., 1997, *ApJ*, 478, 80
- Kaastra, J. S., Mewe, R., Liedahl, D. A., Komossa, S., Brinkman, A. C., 2000, *A&A*, 354L, 83
- Kaastra, J. S., Steenbrugge, K. C., Raassen, A. J., van der Meer, R., Brinkman, A. C., Liedahl, D. A., Behar, E., de Rosa, A., 2002, *A&A*, 386, 427
- Kaspi, S., Brandt, W. N., Netzer, H., Sambruna, R., Chartas, G., Garmire, G. P., Nousek, J. A., 2000, *ApJ*, 535L, 17
- Kaspi, S., & Netzer, H. 1999, *ApJ*, 524, 71
- Kriss, G. A., Green, R. F., Brotherton, M., Oegerle, W., Sembach, K. R., Davidsen, A. F., Friedman, S. D., Kaiser, M. E., Zheng, W., Woodgate, B., Hutchings, J., Shull, J. M., York, D. G., 2000, *ApJ*, 538, 17
- Korista, T. K., Voit, G. M., Morris, S. L., & Weymann, R. J. 1993, *ApJS*, 88, 357
- Proga, D., 2003, *ApJ*, 592, 9
- Savage, B. D. & Sembach, K. R. 1991, *ApJ*, 379, 245
- Scott, J. E., 2004, *ApJS*, 152, 1
- Telfer, R.C., Kriss, G.A., Zheng, W., Davidson, A.F., & Green, R.F. 1998, *ApJ*, 509, 132
- Weymann, R. J., Morris, S. L., Foltz, C. B., & Hewett, P. C. 1991, *ApJ*, 373, 23